Usage of Numerical Optimization in Wind Turbine Airfoil Design

F. Grasso

This paper has been published in Journal of Aircraft, AIAA, Vol.48, No.1, January-February 2011, DOI: 10.2514/1.C031089

ECN-W--11-005 FEBRUARY 2011

JOURNAL OF AIRCRAFT
Vol. 48, No. 1, January–February 2011

Usage of Numerical Optimization in Wind Turbine Airfoil Design

F. Grasso*
Energy Research Centre of the Netherlands, 1755 LE Petten, The Netherlands

DOI: 10.2514/1.C031089

One important key element in the aerodynamic design of wind turbines is the use of specially tailored airfoils to increase the ratio of energy capture to the loading and thereby to reduce the cost of energy. This work is focused on the design of a wind turbine airfoil by using numerical optimization. First, the requirements for this class of airfoils are illustrated and discussed in order to have an exhaustive outline of the complexity of the problem. Then the optimization approach is presented; a gradient-based algorithm is used, coupled with RFOIL solver and a composite Bézier geometrical parameterization. A particularly sensitive point is the choice and implementation of constraints; to formalize the design requirements in the most complete and effective way, the effects of activating specific constraints are discussed. Finally, a numerical example regarding the design of a high-efficiency airfoil for the outer part of a blade is illustrated, and the results are compared with existing wind turbine airfoils.

Nomenclature

α	=	angle of attack, deg
C_d	=	airfoil drag coefficient
$C_{d\,\min}$	=	minimum airfoil drag coefficient
C_f	=	skin-friction coefficient
C_l	=	airfoil lift coefficient
$C_{l\alpha}$	=	slope of the lift curve
$C_{l\,\max}$	=	maximum airfoil lift coefficient
$C_{\mathrm{mc}/4}$	=	airfoil moment coefficient referred to as the quarter-chord
c	=	airfoil chord
F	=	objective function
g	=	inequality constraints
h	=	equality constraints
H	=	boundary-layer shape factor
L/D	=	aerodynamic efficiency
X	=	design variables
X^L	=	lower bounds for the design variables
X^U	=	upper bounds for the design variables

I. Introduction

DESIGN of airfoils specifically suited for wind turbine blade applications is important in the continuing development of wind turbines. In the modern wind turbines, some aviation airfoils such as NACA-63XXX and NACA-64XXX are still quite frequently used, but new airfoil families for wind turbines are increasingly developed because of the intrinsic requirements in terms of design point, offdesign capabilities, and structural properties.

The development of wind turbine airfoils was intensified in the mid-1980s when Tangler and Somers [1] developed numerous airfoils. An overview of available NREL airfoils can be found in [1]. Björk [2] and Timmer and van Rooij [3] have made other significant contributions to this field. The development of the Risø airfoils was initiated in the mid-1990s and has led to the design of three airfoil families [4].

The target design characteristics for the airfoils have been updated during the years and tailored to the specific type of power control and the need for offdesign operation. The desirable airfoil characteristics can be divided into structural and aerodynamic properties, and the wind turbine blade can be divided into the root, middle, and tip parts, where the root part is mainly determined from structural considerations. In contrast, the tip part is determined from aerodynamic considerations.

This work is focused on the design of a wind turbine dedicated airfoil for the tip region of the blade by using numerical optimization. In the next section, the requirements for this class of airfoils are presented, then the used approach is explained. Finally, the design of the new airfoil is described and the results are discussed.

II. Airfoils for Wind Turbines

Airfoil characteristics include both aerodynamic and structural requirements. For the outer part of the blade, the most important parameters from the structural point of view are the maximum airfoil thickness and the chordwise location of the maximum thickness. The thickness of the profile must be able to accommodate the structure necessary for blade strength and stiffness. Depending of the class of the wind turbine, certain values for the thickness along the blade can be expected, and this fact introduces a first indication for the design problem. In the case of a megawatt-class wind turbine, for example, a realistic value for the relative thickness at the tip can be around 18% of the chord. The location of the maximum thickness along the chord is also important; when an airfoil is designed, the other airfoils along the blade should also be considered to guarantee constructive compatibility. This means that in order to allow the spar passing through the blade, the chordwise position of the thickness should be similar for the complete blade.

From the aerodynamic point of view, the most important parameter for the tip region is the aerodynamic efficiency (L/D). To obtain good turbine performance, the aerodynamic efficiency should be as high as possible, but other considerations should be taken into account at the same time. One consideration is related to the stall behavior and the $C_{l\,\max}$. Some of the existing airfoils for wind turbines also have a high value of $C_{l\,\max}$ and a relative high value for the design C_l; this means that for a certain load, a smaller chord is necessary. This reduces loads under parked conditions at high wind speeds. A lower chord in the outboard sections also reduces weight. In addition to this, a high C_l value (and lower associated chord c) in the outboard sections reduces the amplitude of load fluctuations resulting from wind gusts. Hence, a high C_l is desirable to reduce

Presented as Paper 2010-4404 at the 28th AIAA Applied Aerodynamics Conference, Chicago, IL, , 28 June–1 2010; received 28 April 2010; revision received 22 August 2010; accepted for publication 31 August 2010. Copyright © 2010 by Francesco Grasso. Published by the American Institute of Aeronautics and Astronautics, Inc., with permission. Copies of this paper may be made for personal or internal use, on condition that the copier pay the $10.00 per-copy fee to the Copyright Clearance Center, Inc., 222 Rosewood Drive, Danvers, MA 01923; include the code 0021-8669/11 and $10.00 in correspondence with the CCC.

*Postdoctoral Aerodynamicist, Wind Energy Unit, Rotor and Farm Aerodynamics Group, Westerduinweg 3; grasso@ecn.nl, Associate Fellow AIAA.

fatigue and parking loads and can save weight. On the other hand, the stall can be abrupt and undesirable vibrations can be induced on the blade. So it is important that the transition and the separation move gradually when the angle of attack increases. Another important consideration is related to the sensitivity of the airfoil to the roughness. An airfoil with a large laminar flow extension will be very efficient in clean conditions, but very bad in the case of dirty conditions. The $C_{mc/4}$ should also be taken into account, because large values of moment coefficient will give a higher torsion moment on the blade; for pitch-regulated wind turbines, small values for $C_{mc/4}$ mean a reduction in control forces. Also in this case, the other airfoils used on the blade should be considered in order to have a similar value for the moment coefficient; this will prevent the rotor from irregular performances along the blade coming from too-different airfoils. This is one of the reasons why, more than in aviation, the trend in airfoil design is to develop families of airfoils. The last problem that should be taken into account in developing airfoils for wind turbines is connected with gusts. Because of gusts, the local angle of attack for the single airfoil can suddenly change and be in prestall or stall zone. So it is important to keep good offdesign performances and try to have an angle-of-attack range between the design angle of attack and the one for which noticeable separation occurs on the airfoil.

III. Numerical Optimization Approach

To design airfoils, several methodologies can be used. A very popular approach is the Lighthill inverse technique, widely developed by Eppler and Somers [5], Eppler [6], and Drela [7,8]. The basic principle of this design method is that the pressure coefficient on the airfoil surface is prescribed and the airfoil geometry is created; by iteratively modifying the pressure distribution on the airfoil surface, the designer can generate the geometry of an airfoil that satisfies the requirements. Despite its large use, there are several disadvantages associated with this technique; the most evident is that it is very difficult to take multiple requirements into account at the same time, especially when they concern different disciplines.

A valid alternative to solve this problem is the usage of multidisciplinary design optimization (MDO) approach. In the most general sense, numerical optimization [9,10] solves the nonlinear constrained problem to find the set of design variables X_i, for $i = 1, \ldots, N$, contained in vector $\boldsymbol{X}$ that will do the following:

$$\text{Minimize } F(X) \tag{1}$$

subject to

$$g_j(X) \leq 0 \qquad j = 1, \ldots, M \tag{2}$$

$$h_k(X) = 0 \qquad k = 1, \ldots, L \tag{3}$$

$$X_i^L \leq X_i \leq X_i^U \qquad i = 1, \ldots, N \tag{4}$$

Equation (1) defines the objective function, which depends on the values of the design variables, $\boldsymbol{X}$. Equations (2) and (3) are inequality and equality constraints, respectively [equality constraints can be written as inequality constraints and included in Eq. (2)], and Eq. (4) defines the region of search for the minimum. The bounds defined for each degree of freedom by Eq. (4) are referred to as side constraints.

A. Geometry Description

One of the most important ingredients in numerical optimization is the choice of design variables and the parameterization of our system in using these variables. To reduce the number of necessary parameters to take into account to describe the airfoil's shape, but without loss of information about the geometrical characteristics of the airfoil, several mathematical formulations were proposed in literature [11]. In the present work, a composite third-order Bézier is used. Basically, the airfoil is divided in four parts, and a third-order

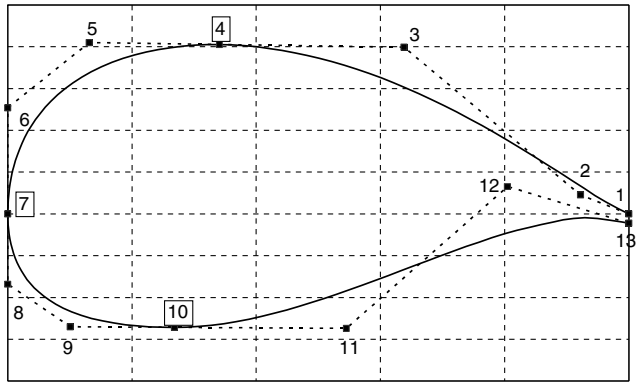

Fig. 1 Geometry parameterization example.

Bézier curve is used to describe the geometry for each part. The advantage of this choice is the possibility to conjugate the properties of Bézier functions in terms of regularity of the curve and easy usage, with a piecewise structure that also allows local modifications to the geometry. The complete description can be found in [12]. A representative sketch is illustrated in Fig. 1, in which the points between 1 and 4 define the first Bézier curve, the points between 4 and 7 define the second curve, and so on. In total, 13 control points are used to describe the airfoil geometry: that means 26 deg of freedom. In practice, however, the leading edge is fixed (control point 7), as is the abscissa of the trailing edge (control points 1 and 13); the abscissas of control points 6 and 8 are also fixed in order to maintain the curvature continuity at the leading edge, and the control points 4 and 10 are directly controlled by the algorithm to keep the curvature continuity between two different Bézier curves. Fourteen degrees of freedom are actively used in the design process.

B. Optimization Algorithm

The choice of optimization algorithm is very important, because the final results are usually dependent on the specific algorithm in terms of accuracy and local minima sensitivity. Evolutionary algorithms are less sensitive to local minima; however, they are time-consuming, and constraints have to be included as a penalty term to the objective function. On the other hand, gradient-based algorithms can lack in global optimality but allow multiple constraints and are more robust, especially for problems in which a large number of constraints are prescribed. In this investigation, the advanced NLPQP gradient-based algorithm from Schittkowski [13] is implemented and the gradients are approximated by finite differences.

C. Objective-Function Evaluation

Since the optimization process requires many evaluations of the objective function and the constraints before an optimum design is obtained, the computational costs and accuracy of the results cannot be neglected. Here, the RFOIL [14] numerical code is used. RFOIL is a modified version of XFOIL [15] featuring an improved prediction around the maximum lift coefficient and capabilities of predicting the effect of rotation on airfoil characteristics. Regarding the maximum lift in particular, numerical stability improvements were obtained by using the Schlichting velocity profiles for the turbulent boundary layer, instead of the Swafford velocity profiles. Furthermore, the shear lag coefficient in Green's lag entrainment equation of the turbulent boundary-layer model was adjusted, and deviation from the equilibrium flow has been coupled to the shape factor of the boundary layer. The following figures illustrate a comparison with experimental data [16] for the NACA-$63_3$418 airfoil. The Reynolds number is 6×10^6 and the transition is free.

It should be noted that the RFOIL prediction for the stall region is well described and very close to the experimental data; in XFOIL results, only the deviation from the linear zone is described, but not the stall. For the drag curve, XFOIL and RFOIL are very close to each other for small values of C_l, but for high C_l, XFOIL underpredicts. In [14], a additional drag of 10% is suggested to correct the RFOIL data;

by adding this factor, a very good agreement is also found for the drag coefficient. To have more realistic predictions, this 10% drag penalty is added during the optimization process (Figs. 2 and 3).

IV. Design of Tip-Region Airfoil

The design of a new airfoil is presented in this section. As anticipated in the previous sections, the requirements for the tip region of the blade are considered. A megawatt-class wind turbine is chosen as the reference. The Reynolds number is 6×10^6 and the airfoil is designed to maximize the aerodynamic efficiency at a 7 deg angle of attack.

The NACA0012 airfoil was used as the baseline for the optimization. The purpose of this choice is to have a starting point for the design process, as far as possible from potential local solutions and, in this way, to have more confidence in the optimality of the solution.

A. Geometrical Constraints

The thickness at the tip is usually between 15 and 18% of the chord; here, a minimum value of 18% is prescribed, and a chordwise location of around 30% of the chord is used in order to be compatible with existing airfoils. As a consequence, it should be noted that because of the 12% thickness, the baseline is even out of the feasible domain.

A minimum trailing-edge thickness of 0.25% of the chord is required to ensure the airfoil's feasibility from a manufacturing point of view.

One of the problems outlined in the previous sections is the insensitivity for the roughness and the need to have a smooth stall, with gradual transition and separation. By using the results of the Engineering Sciences Data Unit [17] and the extension from Gault [18], a minimum value for the ordinate at x/c equal to $0.0125c$ can be selected to ensure a trailing-edge separation. From this parameter, a minimum leading-edge radius of $0.015c$ can be assigned. The main advantage of this choice is the fact that the stall is included in the design process by connecting it to a geometrical parameter; this means that the result is not affected by eventual numerical inaccuracy and it is not necessary to perform aerodynamic analyses at stall conditions. However, due to the importance of the stall behavior and in order to do not force the solution by restricting the domain too much, it is preferred to take into account the stall characteristics by introducing an aerodynamic constraint.

B. Aerodynamic Constraints

To limit the blade torsion, a minimum value for $C_{mc/4}$ of -0.08 is prescribed. This value comes from a comparative analysis on experimental data [3,16] for existing airfoils that is realistically usable for this class of turbines. The geometries considered are the DU-W2-401, DU-W2-350, DU97-w-300, DU-W2-250, and NACA-$63_4$421 (Figs. 4 and 5). It should be noted that apart from the DU-W2-250 airfoil, the chosen value for the moment coefficient is reasonable.

Regarding the problems related to the gusts, a minimum range of 7 deg is required between the design angle of attack and the start of significant separation. This is done by imposing that the position of the separation point on the suction side, based on the shape factor H being equal to 2.8, is a minimum of 90% of the chord at an angle of attack equal to 14 deg.

To avoid the possibility of abrupt stall and to converge to a solution in which a Stratford-style recompression is not present (it can lead to a not-gradual evolution in transition location), the design is performed by fixing transition at $0.01c$ on the suction side and $0.1c$ on the pressure side. The optimization process in fixed-transition conditions, together with the above-mentioned constraint related to the location of the separation, should give reasonably good results about stall characteristics. The drawback of this solution is the increase in time of the optimization process, due to the fact that for each iteration, the complete lift curve up to the stall condition needs to be calculated to ensure the accuracy of results and not just the design condition.

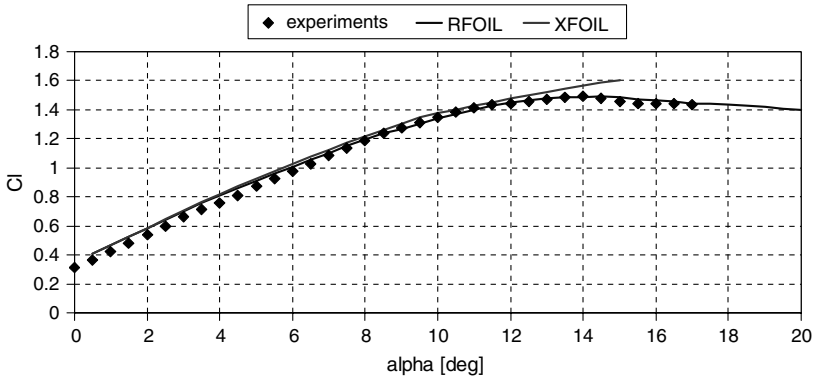

Fig. 2 Lift curve for the NACA-$63_3$418 airfoil; comparison between XFOIL and RFOIL with experiments [16]; $Re = 6 \times 10^6$; and free transition.

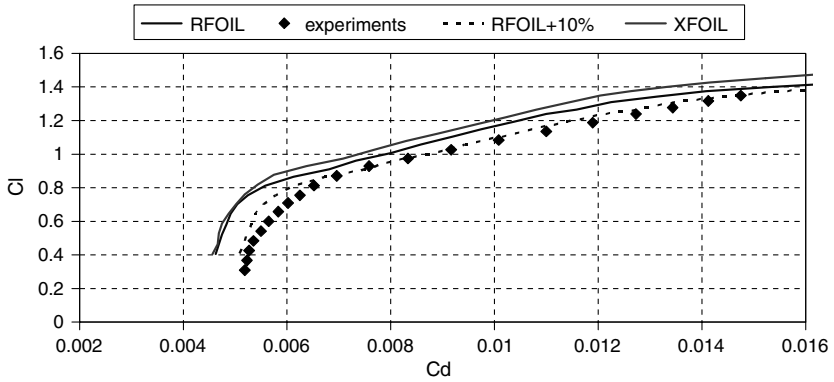

Fig. 3 Drag curve for the NACA-$63_3$418 airfoil; comparison between XFOIL and RFOIL with experiments [16]; $Re = 6 \times 10^6$; and free transition.

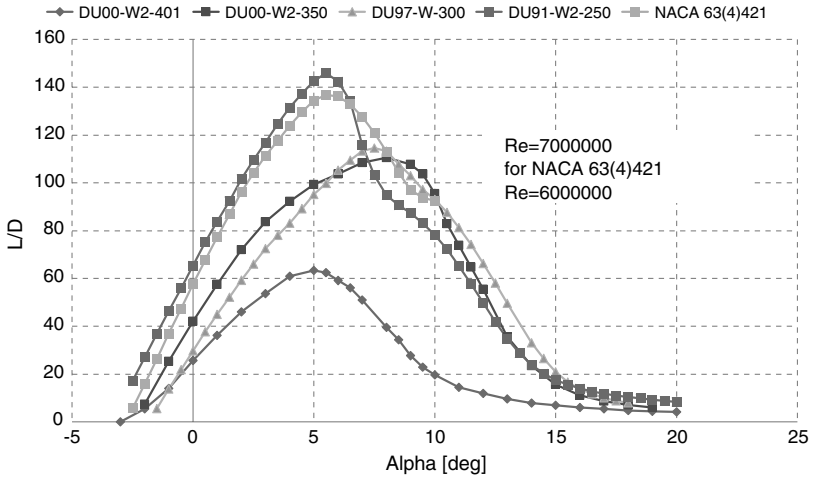

Fig. 4 Efficiency curve for selected airfoils at $Re = 6 \times 10^6$ ($Re = 7 \times 10^6$ for NACA$63_4$421). Experimental data [3,16].

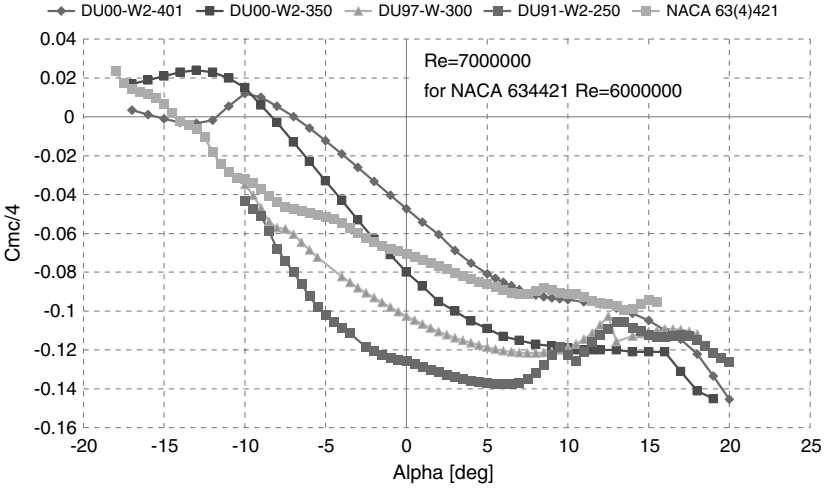

Fig. 5 Moment coefficient curve for selected airfoils at $Re = 7 \times 10^6$ ($Re = 6 \times 10^6$ for NACA$63_4$421). Experimental data [3,16].

C. Results

Figure 6 shows the comparison between the new airfoil, named GWA1-18, and the NACA$63_3$418, NACA$64_3$418, NACA$63_3$618, and NACA$64_3$618 airfoils.

In Figs. 7 and 8, the aerodynamic characteristics are compared. A value for the maximum efficiency greater than 150 is reached, achieving a good offdesign performance at the same time, especially if compared to the peaky performances of NACA airfoils. In the figures the experimental data are also used to show the general reliability of RFOIL. In the absence of wind-tunnel tests, this fact should give some confidence about the robustness of the GWA1-18 airfoil data. The moment coefficient is respecting the imposed bound as well as the separation that occurs after the stall at 15 deg (Fig. 9). Looking at the lift-coefficient curve, it can be seen that good high-lift characteristics have been obtained with a not-abrupt stall. The high-lift characteristics allow reducing the chord, so it is beneficial to design a slender and lighter blade, also reducing the loads along the blade. Because of the large extension of the linear region of the lift curve, the slope of the curve is constant up to the stall. This means that the fatigue loads, due to variation of C_l and thus of $C_{l\alpha}$, will also be reduced (Figs. 10–12).

1. *Effects of Roughness*

The airfoils are also compared by simulating the presence of roughness; the analysis was performed by imposing the transition at $0.01c$ on the top surface and at $0.1c$ on the lower surface. It should be noted that the performance of the GWA1-18 in dirty conditions is

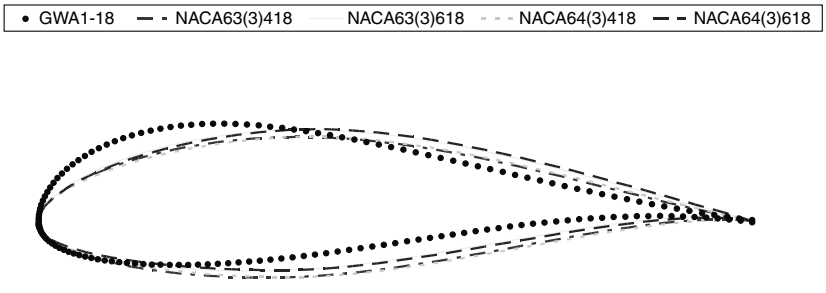

Fig. 6 GWA1-18 airfoil compared with NACA geometries.

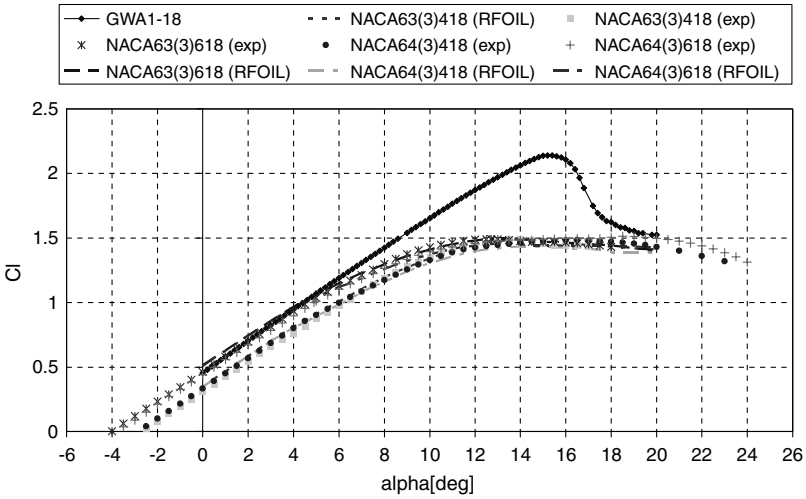

Fig. 7 Lift-coefficient curve; comparison between the GWA1-18 and NACA airfoils at $Re = 6 \times 10^6$, free transition, and RFOIL predictions; experimental data from Abbott [16].

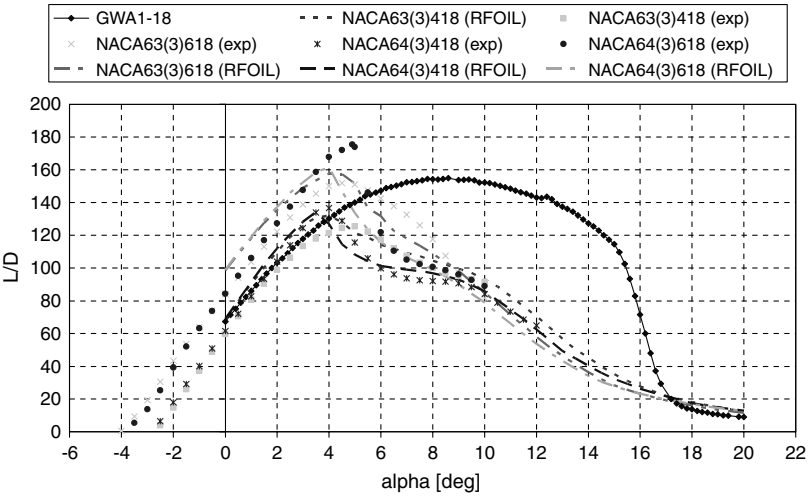

Fig. 8 Efficiency curve; comparison between the GWA1-18 and NACA airfoils at $Re = 6 \times 10^6$, free transition, and RFOIL predictions; experimental data from Abbott [16].

better than the NACA airfoils performance, and the loss in efficiency due to the imposed transition is less than for the NACA geometries (Fig. 13). An interesting consideration can be addressed in terms of the design point. Because of the good offdesign characteristics of the GWA1-18 airfoil, the angle of attack at which the maximum efficiency is reached is almost the same in clean and dirty conditions. For the NACA airfoils, the change in optimal condition is more evident; as a consequence, the safety margin for gusts is significantly reduced.

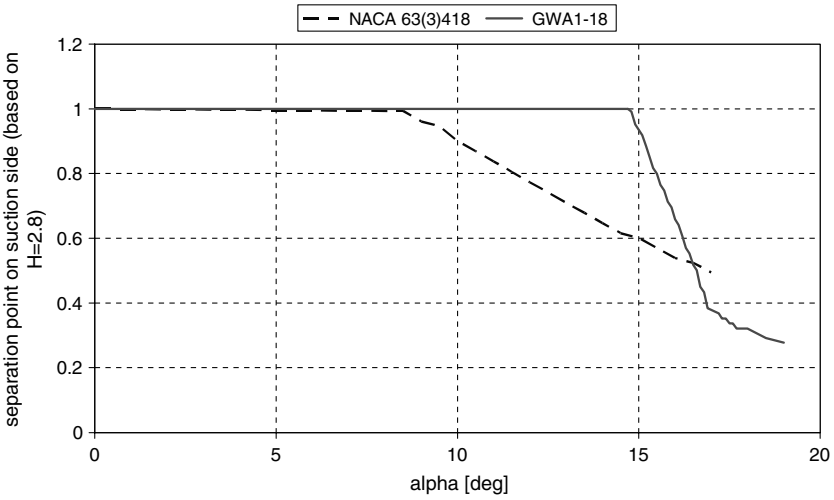

Fig. 9 Separation evolution by varying the angle of attack for the GWA1-18 airfoil; RFOIL predictions based on $H = 2.8$.

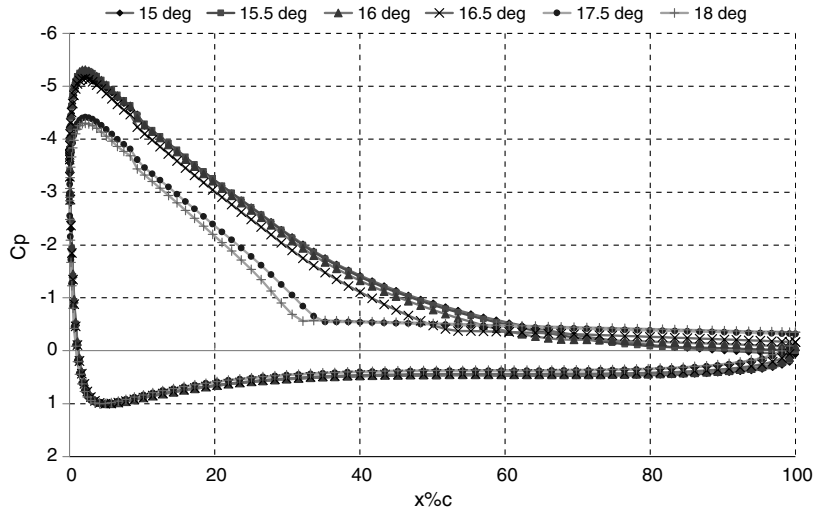

Fig. 10 10 Pressure-coefficient distribution on GWA1-18 airfoil; RFOIL predictions, $Re = 6 \times 10^6$, and free transition.

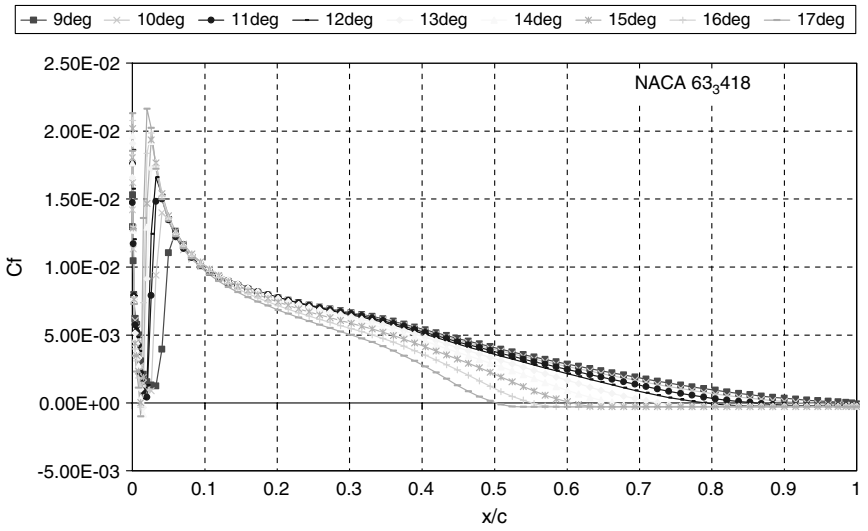

Fig. 11 C_f change due to the angle of attack for the NACA63$_3$418 airfoil; RFOIL predictions, $Re = 6 \times 10^6$, and free transition.

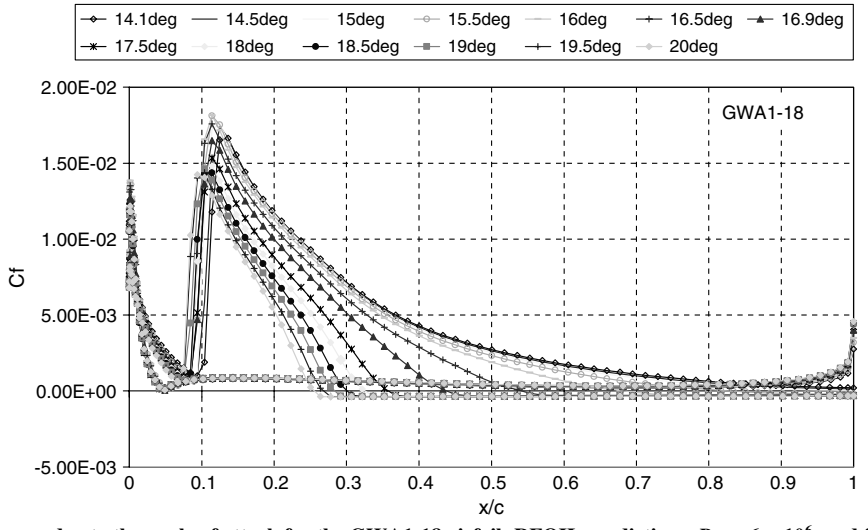

Fig. 12 C_f change due to the angle of attack for the GWA1-18 airfoil; RFOIL predictions, $Re = 6 \times 10^6$, and free transition.

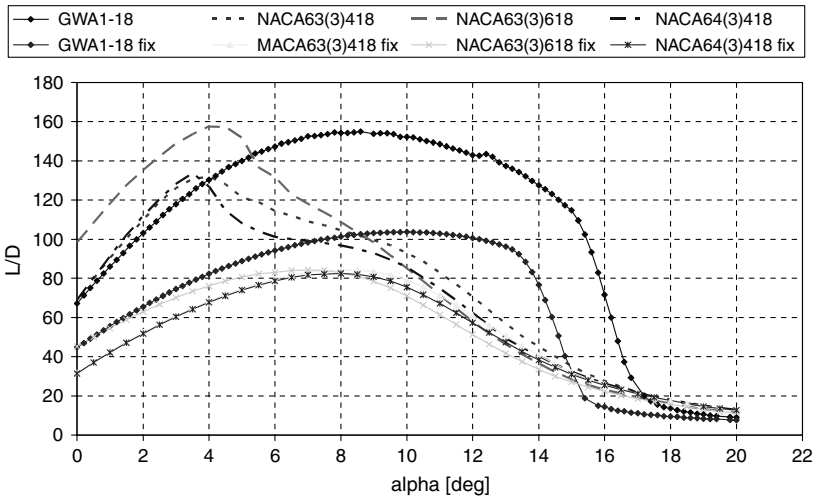

Fig. 13 Lift-coefficient curve; comparison between the GWA1-18 and NACA airfoils at $Re = 6 \times 10^6$; RFOIL predictions; effect of imposed transition.

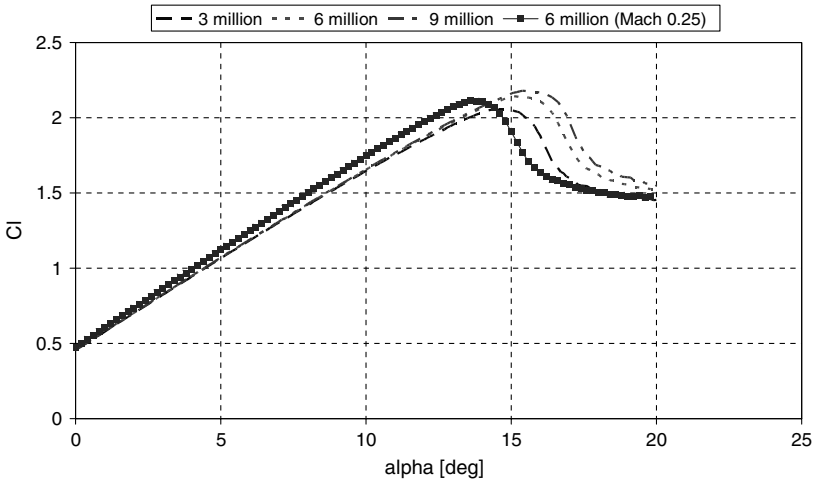

Fig. 14 Lift-coefficient curve for the GWA1-18 airfoil; Reynolds number and Mach number effects, RFOIL calculations, and free transition.

2. Effects of Reynolds Number and Mach Number

The effect related to the Reynolds number has been analyzed. The characteristics of the lift curve and the efficiency curve do not change sensibly; the characteristics at stall and the shape of the efficiency curve are just scaled because of the Reynolds number.

During the design process, the flow is assumed to be incompressible; however, for real megawatt-class wind turbines, the velocity at the tip of the blade can reach 90–100 m/s: that means a Mach number equal to 0.25–0.3. In Figs. 14 and 15, the effects due to the Reynolds and Mach numbers are shown. According to the RFOIL predictions, the main effects due to the compressibility are an increment in drag at high angles of attack and a shift of the lift curve, but the characteristics of the GWA1-18 airfoil in terms of stall and efficiency characteristics are still good.

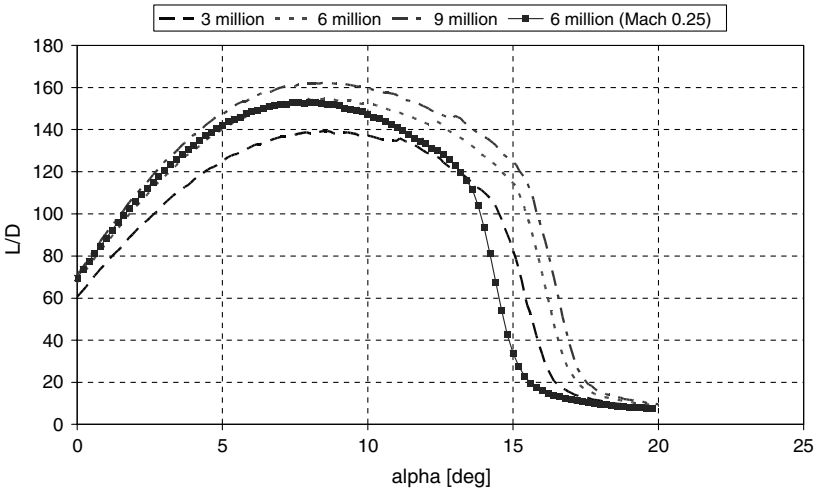

Fig. 15 Efficiency curve for the GWA1-18 airfoil; Reynolds number and Mach number effects; RFOIL calculations; free transition.

In the absence of experimental data, the stall characteristics have been compared with the above-mentioned work from Gault [18]; according to these data, the stall for the GWA1-18 airfoil is expected to be due to trailing-edge separation.

V. Conclusions

A new airfoil for wind turbines was designed. According to the RFOIL predictions, the results are promising when compared with commonly used NACA airfoils. A very good value for the efficiency was achieved, with separation limited only in the stall zone. The high value for the C_l can be valuable to reduce chord, and thus loads and weight, to the tip of the blade. Because of the relatively large leading-edge radius, the performances in offdesign and rough conditions are also good. The stall, even if not as long as for the NACA airfoils, is also quite smooth if the high-lift character of the GWA1-18 airfoil is considered.

Despite these good results, wind-tunnel tests are recommended to validate predictions. Especially for the stall behavior, the numerical predictions (and, consequently, the MDO process used in this work) need to be verified.

Acknowledgment

The author would like to thank H. Snel for the precious help and suggestions during this work.

References

[1] Tangler, J. L., and Somers, D. M., "NREL Airfoil Families for HAWT's," *WINDPOWER '95*, Washington, D.C., 1995, pp. 117–123.

[2] Björk, A., "Coordinates and Calculations for the FFA-W1-xxx, FFA-W2-xxx and FFA-W3-.xxx Series of Airfoils for Horizontal Axis Wind Turbines," FFA, Aeronautical Research Inst. of Sweden, TN 1990-15, Stockholm, 1990.

[3] Timmer, W. A., and van Rooij, R. P. J. O. M., "Summary of the Delft University Wind Turbine Dedicated Airfoils," AIAA Paper 2003-0352, 2003.

[4] Fuglsang, P., and Bak, C., "Design and Verification of the New Risø-A1 Airfoil Family for Wind Turbines," AIAA Paper 2001-0028, 2001.

[5] Eppler, R., and Somers, D. M., "A Computer Program for the Design and Analysis of Low-Speed Airfoils," NASA TM-80210, 1980.

[6] Eppler, R., *Airfoil Design and Data*, Springer–Verlag, Berlin, 1990.

[7] Drela, M., "XFOIL: An Analysis and Design System for Low Reynolds Number Airfoils, Conference on Low Reynolds Number Airfoil Aerodynamics," Univ. of Notre Dame, Notre Dame, IN, June 1989.

[8] Drela, M., and Giles, M. B., "Viscous-Inviscid Analysis of Transonic and Low Reynolds Number Airfoils," *AIAA Journal*, Vol. 25, Oct. 1987, pp. 1347–1355. doi:10.2514/3.9789

[9] Fletcher, R., *Practical Methods of Optimization*, Wiley, New York, 1987.

[10] Pedregal, P., *Introduction to Optimization*, Springer, New York, 2004.

[11] Samareh, J. A., "Survey of Shape Parameterization Techniques for High-Fidelity Multidisciplinary Shape Optimization," *AIAA Journal*, Vol. 39, No. 5, May 2001, pp. 877–884. doi:10.2514/2.1391

[12] Grasso, F., "Multi-Objective Numerical Optimization Applied to Aircraft Design," Ph.D. Thesis, Aerospace Engineering, Università di Napoli Federico II, Napoli, Italy, Dec. 2008.

[13] Schittkowski, K., "NLPQLP: A New Fortran Implementation of a Sequential Quadratic Programming Algorithm—User's Guide, Version 1.6," Dept. of Mathematics, Univ. of Bayreuth, Bayreuth, Germany, 2001.

[14] van Rooij, R. P. J. O. M., "Modification of the Boundary Layer Calculation in RFOIL for Improved Airfoil Stall Prediction," Delft Univ. of Technology Rept. IW-96087R, Delft, The Netherlands, Sept. 1996.

[15] Drela, M., "XFOIL 6.94 User Guide," Aeronautics and Astronautics Dept., Massachusetts Inst. of Technology, Cambridge, MA, Dec. 2001.

[16] Abbott, I., Von Doenhoff, A., "Theory of Wing Sections," Dover, New York, 1958.

[17] " The Low-Speed Stalling Characteristics of Aerodynamically Smooth Airfoils," Engineering Sciences Data Unit, Rept. ESDU 66034, London, Oct. 1966.

[18] Gault, D. E., "A Correlation Of Low-Speed Airfoil-Section Stalling Characteristics with Reynolds Number and Airfoil Geometry," NACA TN 3963, March 1957.